JOURNAL OF GEOPHYSICAL RESEARCH, VOL. 92, NO. A9, PAGES 9963-9970, SEPTEMBER 1, 1987

THE INTERACTION OF IO'S ALFVEN WAVES WITH THE JOVIAN MAGNETOSPHERE

Andrew N. Wright

Theoretical Astronomy Unit, School of Mathematical Sciences,
Queen Mary College, London

Abstract. A numerical solution for the propagation of the Alfvén waves produced by Io is presented. The waves are shown to interact strongly with the torus and magnetic field inhomogeneities. We find substantial reflection occurs from the magnetospheric medium and only about a quarter of the wave power will reach the ionosphere on its first pass. It is concluded that both WKB and ray tracing arguments are inappropriate, contrary to previous studies. A more realistic picture may be that of a whole field line or L shell resonating in an eigenmode. We discuss the Alfvén structure behind Io and comment upon some possible features that it may exhibit. In particular it may be possible to produce decametric arcs that are more closely spaced than ray tracing permits by exciting higher harmonic eigenmodes of Io's L shell.

Introduction

The interaction of Io with the Jovian magnetosphere has been of particular interest ever since Bigg [1964] discovered the influence of Io upon decametric radiation (DAM) emissions. It is thought that Io or its ionosphere is a good electrical conductor and can be expected to produce large-amplitude Alfvén waves through the mechanism outlined by Drell et al. [1965]. Goertz and Deift [1973] and Neubauer [1980] have both modeled the structure of the waves produced by Io. Wright and Southwood [1987] have presented a general discussion of Alfvén waves and give a more detailed description of these waves than previous studies. The magnetic field observed near the Io flux tube (IFT) by Voyager 1 is in excellent agreement with the Alfvén wave model [Acuña et al., 1981; Belcher et al., 1981; Barnett, 1986]. In addition to producing observable signatures in the magnetic field the Alfvén waves also perturb the motion of energetic electrons and ions past the satellite [Schulz and Eviatar, 1977]. Goldstein and Ip [1983] and Wright [1987] have shown how the Voyager 1 10-MeV electron data reported by Lanzerotti et al. [1981] are modified by the presence of the satellite wake. The whole interaction may be more complicated if there exists a tail behind Io where newly ionized particles are accelerated up to the background flow speed [Southwood and Dunlop, 1984].

The original discovery of Bigg [1964] prompted Goldreich and Lynden-Bell [1969] to suggest the DAM emissions were produced within the Io flux tube. Warwick et al. [1979a,b] observed arclike structures in the frequency-time spectrograms of Voyager 1 and 2. They noted, *en passant*, that a similar pattern would be observed if DAM emissions were produced near the local electron gyrofrequency and beamed along the surface of cones. They also argued that the repeatability of the arcs suggested a geometrical explanation. Clearly the manner in which Io's Alfvén waves propagate through the torus will be essential in understanding the Voyager observations.

Neubauer [1980] noted that the change in plasma density seen by the wave as it propagates through the torus may produce some reflections. This would give rise to a particularly complex pattern of waves behind Io as there are certain to be reflections from the Jovian ionosphere also [Gurnett and Goertz, 1981]. Walker and Kivelson [1981] found evidence for the existence of a current structure on Io's L shell in the Pioneer 10 magnetometer data. Fluctuations in the magnetic field were observed well downstream from Io ($\sim 55^\circ$ longitude). The pattern is further complicated by the fact that Io is not confined to the magnetic equator, and the torus may not be independent of longitude. Gurnett and Goertz [1981] argued that reflections from the torus boundary could be neglected because the scale of the wave was small compared with the scale length of the torus. Their estimate of wave size was similar to that of Io. This is actually the perpendicular scale and is considerably smaller than the parallel wavelength, which is more relevant to the nature of wave propagation. Goertz [1980] also concluded that there would be negligible reflection from the torus boundary. However, his calculation was not for a pulse launched from Io but for a harmonic disturbance at the equator. Such a calculation is useful for estimating the heating of the torus, but it is difficult to comment on the propagation features of the waves from this result. His calculation also neglected the geometry of the magnetic field.

Within the WKB limit (no reflection from the torus) Bagenal [1983] calculated the pattern of Alfvén waves produced behind Io in an effort to explain the arc spacing within the framework suggested by Gurnett and Goertz [1981]. Bagenal's work provided plots of Alfvén wave trajectories around Jupiter and is useful for interpreting the spacing of the decametric arcs within the WKB limit.

In this paper we study, numerically, the propagation of Alfvén waves through the Io torus. It is shown that the WKB limit is not valid for Io's Alfvén waves and that the waves strongly interact with the torus. The effect of this interaction will be to produce more complicated wave patterns behind Io, and we discuss the possible new features we may expect.

The Propagation of Alfvén Waves Through a Nonuniform Plasma and Magnetic Field

The nature of wave propagation through an inhomogeneous medium can be classified, to some extent, by the ratio of the wave and medium scale lengths. For example, if the scale length of the medium is much smaller than a wavelength, the inhomogeneity will be well approximated as a discontinuity. Consider a plane wave propagating from a uniform region 1 to a uniform region 2 via a discontinuity in Alfvén speed. There will be transmitted and reflected components from the incident wave. It is easy to show (from continuity of electric and magnetic fields across the discontinuity) that the ratio of transmitted and reflected magnetic field amplitudes relative to the incident amplitude is

$$\begin{array}{ll} \text{Transmitted} & 2V_{A1}/(V_{A1}+V_{A2}) \\ \text{Reflected} & (V_{A1}-V_{A2})/(V_{A1}+V_{A2}) \end{array} \qquad (1)$$

Paper number 6A8855.
0148-0227/87/006A-8855$05.00

where V_A is the local Alfvén speed ($=B/(\mu_0\rho)^{\frac{1}{2}}$) and subscripts 1 and 2 denote quantities in regions 1 and 2 respectively [see Alfvén and Falthammar, 1963]. If the permeability and magnetic field strength do not change across the discontinuity, the reflection and transmission coefficients are determined solely by the change in density;

$$\text{Transmitted} \quad 2\rho_2^{\frac{1}{2}}/(\rho_2^{\frac{1}{2}}+\rho_1^{\frac{1}{2}})$$
$$\text{Reflected} \quad (\rho_2^{\frac{1}{2}}-\rho_1^{\frac{1}{2}})/(\rho_2^{\frac{1}{2}}+\rho_1^{\frac{1}{2}}) \tag{2}$$

For a propagating Alfvén wave the magnetic and velocity field perturbations (b and u) are related to one another by

$$u = \pm\, b/(\mu_0\rho)^{\frac{1}{2}} \tag{3}$$

The plus and minus signs describe propagation antiparallel and parallel to the magnetic field direction. The expression in (2) tells us that a wave incident upon a massive boundary ($\rho_2>>\rho_1$), for example an ionosphere, is perfectly reflected. The magnetic field perturbation is reflected in the same sense as the incident wave; however, (3) shows that the velocity perturbation has the opposite phase to the incident velocity. The opposite extreme ($\rho_1>>\rho_2$) is reminiscent of reflection from a "free end." In this limit it is the reflected magnetic field that changes phase, while the velocity disturbance is reflected in the same sense. Although the transmission coefficient for both $\rho_2>>\rho_1$ and $\rho_1>>\rho_2$ coupled with (3) suggests there may be some transmitted wave, we find that either the velocity perturbation ($\rho_2>>\rho_1$) or the magnetic field disturbance ($\rho_1>>\rho_2$) is zero, and hence there is no Poynting flux in region 2. (The Poynting flux in a transverse Alfvén wave is defined as $-$ (u.b)B_0/μ_0 where B_0 is the background magnetic field.) The total power flow in a wave is the product of the Poynting flux with the cross section of the flux tube. Since the cross section varies inversely with B_0, the power in a wave is proportional to u.b. The expressions in (1) and (3) can be combined to give energy transmission and reflection coefficients (C_T and C_R):

$$C_T = \frac{4\, V_{A1}V_{A2}}{(V_{A1}+V_{A2})^2}$$
$$C_R = \frac{(V_{A1}-V_{A2})^2}{(V_{A1}+V_{A2})^2} \tag{4}$$

where $C_T + C_R = 1$.

In contrast to the above discussion we can consider the case when the wavelength is much smaller than the scale that the plasma varies on. In this limit the medium changes negligibly over one wavelength and appears quasi-uniform to the wave. One may anticipate that there will be no reflection; however, the transmission is not identical to propagation in a uniform medium. Suppose that the medium is represented by a fine series of slabs orthogonal to $\mathbf{B}_0$. In the limit as $\rho_1 \to \rho_2$ across each slab, (1) to (4) tell us that the wave is in fact completely transmitted and that there is no reflected wave. If we assume that the density changes by $\Delta\rho$ in a distance ΔS and that the amplitude of the magnetic field perturbations (A) changes by ΔA, then (using (2))

$$\frac{\Delta A}{A} = \frac{2(\rho+\Delta\rho)^{\frac{1}{2}}}{(\rho+\Delta\rho)^{\frac{1}{2}}+\rho^{\frac{1}{2}}} - 1 = \frac{\Delta\rho}{4\rho} \tag{5}$$

On integrating (5) and using (3) we find

$$b \;\alpha\; \rho^{\frac{1}{4}} \qquad u \;\alpha\; \rho^{-\frac{1}{4}} \tag{6}$$

which is the familiar WKB limit [see Alfvén and Falthammar, 1963]. These two extreme limits are useful for putting upper and lower bounds on the expected behavior of wave propagation even if neither one is strictly applicable.

Previous studies of Alfvén wave propagation from Io have used both of these limits. The wave is commonly assumed to propagate through the Io torus in a similar fashion to the WKB limit (i.e., complete transmission and negligible reflection). When this wave reaches the Jovian ionosphere, the change between the magnetospheric and ionospheric mediums occurs very abruptly on the scale of a wavelength. This is well described by a discontinuity with $\rho_2>>\rho_1$. As we have discussed, this will completely reflect the wave and invert the sense of the velocity disturbance. (Gurnett and Goertz [1981] note that the good electrical conductivity of Jupiter's ionosphere will also reflect the wave.) In order to decide whether or not these assumptions are reasonable we need to estimate the relative sizes of the wave and medium scale lengths in the torus, in the magnetosphere and at the top of the ionosphere.

Relevant Scale Lengths

It is possible to estimate the scale of the Alfvén wave produced by Io if we assume that it is only excited on a field line when it is in contact with the satellite. The convection speed of field lines relative to Io is 57 km s^{-1}, and the satellite radius is R_I = 1.82 × 10^3 km, suggesting an encounter time of 60 s. The Alfvén speed at the center of the torus is about 400 km s^{-1}, which gives a length along the field line of 2.4 × 10^4 km or 0.34 R_J (one Jovian radius, R_J = 7.14 × 10^4 km). These quantities are taken from Dessler [1983]. We shall consider this wavelength as being typical of the Alfvén waves launched from Io. If the waves are excited in the immediate vicinity of Io (e.g., its ionosphere or tail), the wavelength will be greater than 0.34 R_J. It is also possible that the current from Io is quite localized and does not join with Alfvén waves over the entire surface of the satellite. In this case the parallel wavelength may be smaller than 0.34 R_J. In either case the Alfvén speed increases (monotonically) by at least 2 orders of magnitude along Io's L shell and will result in a parallel wavelength above the Jovian ionosphere of the order of hundreds of Jovian radii.

The scale length of the medium is dependent upon the change in magnetic field and density. The torus is thought to have a density scale length of the order of 1 R_J and is centered near the magnetic equator. The scale length of the magnetic field ($B/\nabla B$) is very large near the equator and decreases to about 0.5 R_J above the ionosphere. From these estimates we expect the wavelength and scale length of the medium to be of a similar size when propagating through the Io torus. Outside the torus the medium changes in a discontinuous fashion on the scale of a wavelength. Contrary to previous studies we do not expect the WKB limit (small wavelength) to be valid anywhere (except very close to the magnetic equator where the field and density both have infinite scale lengths). Outside the torus and at the Jovian ionosphere the long wavelength limit should be a reasonable approximation. For these reasons we have chosen to model the propagation of Alfvén waves through the Io torus numerically.

The Numerical Model

The purpose of the model we present here is to study the propagation features of Alfvén waves from Io in the

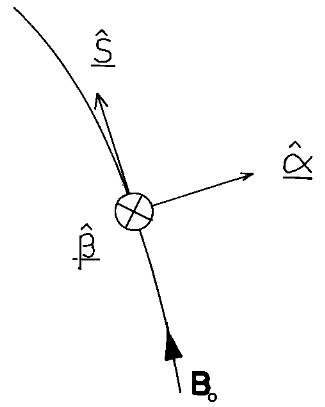

Fig. 1. The coordinate system used for the simulation: $\hat{S}$ lies along the magnetic field direction, $\hat{\beta}$ is oriented azimuthally and $\hat{\alpha}$ completes the right-handed triad (α,β,S).

region where the wavelength and medium scale length are of comparable order. We shall adopt a curvilinear coordinate system (α,β,S) where $\hat{S}$ is parallel to the magnetic field direction, $\hat{\alpha}$ lies in a meridian pointing outward and $\hat{\beta}$ is oriented azimuthally to complete the right-handed triad. The analysis is further simplified by treating the linear limit of the cold plasma equations ($\beta \sim 10^{-3}$). By allowing the triad (α,β,S) to maintain the orientation described above to the magnetic field along the entire length of the field line (see Figure 1) we are able to incorporate the dipole geometry of the field into our model. This enters the equations as geometric factors such as h_α, which is defined as $h_\alpha = \hat{\alpha}/\nabla\alpha$ (cf. introductory vector analysis books [e.g., Davis and Snider, 1979]). Singer et al. [1981] and Southwood and Hughes [1983] have used this coordinate system previously, and the following derivation is similar to their work. Since α and β are constant on a magnetic field line, they may be taken as proportional to the Euler potentials of the magnetic field.

We shall consider the motion of the field lines on Io's L shell. These field lines pass through the center of Io and only experience an azimuthal ($\hat{\beta}$) perturbation to field and velocity. The perturbations are $\mathbf{b} = b\hat{\beta}$; $\mathbf{u} = u\hat{\beta} = \partial\xi/\partial t$; $\xi = \xi\hat{\beta}$; and $\hat{\beta} = h_\beta \nabla\beta$.

The curl E Maxwell equation and Ohm's law for an infinitely conducting plasma give

$$\frac{\partial \mathbf{b}}{\partial t} = \nabla_\wedge(\mathbf{u}_\wedge \mathbf{B}_0) = \nabla_\wedge\left[\frac{\partial \xi}{\partial t} B_0\, \hat{\alpha}\right] \tag{7}$$

After a little algebra we find

$$\frac{\partial b}{\partial t} = \frac{1}{h_\alpha}\frac{\partial}{\partial S}\left[\frac{\partial \xi}{\partial t} h_\alpha B_0\right] \tag{8}$$

The momentum equation is

$$\rho\, \frac{\partial^2 \xi}{\partial t^2} = \mathbf{j}_\wedge \mathbf{B}_0 = (\nabla_\wedge \mathbf{b})_\wedge \mathbf{B}_0/\mu_0 \tag{9}$$

After similar manipulations to that following (7) we get

$$\mu_0\, \rho\, \frac{\partial^2}{\partial t^2}(\xi\hat{\beta}) = \hat{\beta}\, \frac{B_0}{h_\beta}\frac{\partial}{\partial S}(b h_\beta) \tag{10}$$

Equations (8) and (10) are the two coupled, linear plasma equations whose solutions we give. When these are written in terms of b and u alone, we have

$$\frac{\partial b}{\partial t} = \frac{1}{h_\alpha}\cdot\frac{\partial}{\partial S}(u h_\alpha B_0)$$
$$\frac{\partial u}{\partial t} = \frac{B_0}{\mu_0 \rho h_\beta}\frac{\partial}{\partial S}(h_\beta b) \tag{11}$$

These equations are discussed in the appendix where we show that either they describe a one-dimensional toroidal oscillation ($\partial/\partial\alpha = \partial/\partial\beta = 0$) of the entire L shell, or the wave satisfies $\nabla.(B_0 u_\perp) = 0$ in which case we can describe a single field line motion. Both of these conditions require the magnetic field perturbation to be perpendicular to the magnetic field, and this was indeed observed to be the case at Io by Acuña et al. [1981] and also downstream from Io by Walker and Kivelson [1981]. The Jovian magnetic field deviates from a dipolar field by about 10% at Io's L shell [Acuña et al., 1983]. We shall neglect this small difference and use a dipole field geometry. For a dipole background magnetic field the factors h_α and h_β are defined as [Singer et al., 1981]

$$h_\alpha = 1/(r B_0 \cos\lambda)$$
$$h_\beta = r\cos\lambda \tag{12}$$

The (r,λ,z) coordinates are shown in Figure 2. It is necessary to assume a form for the distribution of plasma density along the L shell, and we have taken the following form (based upon the plasma instrument on Voyager 1 [Bagenal et al., 1985; F. Bagenal, private communication, 1986]):

$$\rho(\text{amu/cm}^3) = (4.73\times10^4)\exp[-(z/1R_J)^2] \quad \lambda < 35.3^\circ$$
$$\rho(\text{amu/cm}^3) = 267.7 \quad \lambda > 35.3^\circ \tag{13}$$

This density profile is plotted in Figure 3. Because of the present uncertainty in the ratio of parallel and perpendicular temperatures the plasma may be distributed along the field line more evenly than in our model, or even confined more closely to the equator. However, the profile in (13) is thought to be reasonable from data currently available. Inspection of Figure 3 shows the density scale length $(\partial\ln(\rho)/\partial s)^{-1}$ to be infinite at $S = 0$ and $S > 4\ R_J$. In between, the scale length assumes smaller values around $1\ R_J$ for $0.5 < S/R_J < 3$. (The smallest scale length is $0.55\ R_J$ and occurs at $S = 1.6\ R_J$.)

The boundary conditions are, of course, very important in determining the behavior of the solution to (11). By assuming that Io and the center of the torus coincide with the magnetic equator the problem is sufficiently symmetric to only consider one half of the L shell, or field line. The boundary condition that we impose at the equator is b = 0. This is because the wave structure above Io will have the opposite magnetic field disturbance to the

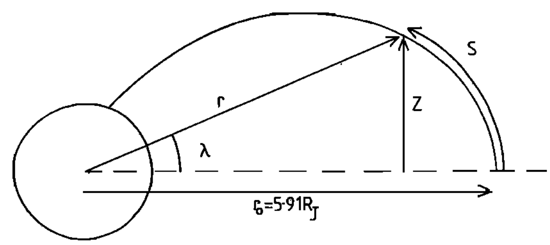

Fig. 2. The dipolar magnetic field line for Io's L shell. The coordinates (r,λ,z) are also shown.

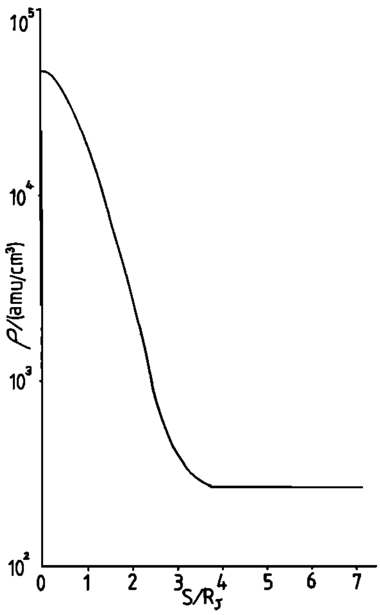

Fig. 3. The variation of plasma density along Io's L shell. The plasma is largely sulfur and oxygen ions within the dense torus and hydrogen ions at higher latitudes.

structure below, and combining both halves gives zero perturbation at the exact position of the equator. This saves computer usage by requiring us to solve the equations on only half of the field line. The boundary conditions at the ends of the field line can be chosen depending upon what feature of the system we wish to investigate. One reasonable choice would be a perfectly reflecting ionosphere ($u = 0$). This would reflect the wave reaching the ionosphere back toward the torus where there may be subsequent reflection and transmission by the inhomogeneous medium. Another choice is to have a perfectly absorbing end to the field line, i.e., one that absorbs the wave completely and produces no reflection. In order to focus on the manner in which the wave interacts with the medium as it propagates through it, and not so much on any bouncing structure that is set up, we have chosen the latter condition. The advantage of using a perfectly absorbing ionospheric end to the field line is that any reflection that does occur will be due to inhomogeneities in the medium (i.e., the density and magnetic field). Including reflection from the ionosphere would make the interpretation of the simulation results more difficult. The perfectly absorbing end of the field line is achieved by suppressing reflection from the last grid point.

The only remaining boundary condition is the form of the source. We have chosen the following disturbance to be introduced at $S = 0^+ R_J$:

$$u = u_{on}[1 - \cos(2\pi t/T)]/2 \qquad 0 < t < T$$
$$u = 0 \qquad t > T \tag{14}$$
$$b = - u[\mu_0\rho(0)]^{\frac{1}{2}}$$

This wave has a duration T and propagates parallel to the magnetic field direction. This form for the wave was chosen because it is a smooth, well-behaved function. Note that this magnetic field perturbation is actually enforced at $S = 0^+$. At $S = 0$, symmetry requires $b = 0$. In the case of a very long period wave ($T \gg 1$) there will be some reflected wave at $S = 0$ while the perturbation due to Io (equations (14)) is still finite. This does not occur for $T < 1.4$. However, it will occur for large T and is accommodated in the program by superposing (14) upon whatever reflection may be present at $S = 0^+$.

The integration technique that was used to solve the equations was the two-step Lax-Wandroff method. This is a finite difference scheme that is accurate to second order.

Computational Results

Throughout the rest of this paper normalized units are used, unless stated otherwise. The units are length, one Jovian radius ($1\ R_J = 7.14\times10^4$ km); velocity, the equatorial Alfvén speed ($V_{Aeq} = 400$ km s^{-1}); and time, the equatorial Alfvén travel time ($1\ R_J/V_{Aeq} = 180$ s). The program was run as described in the previous section with a variety of values for T spanning 2 orders of magnitude and centered on the predicted value of 0.34. The equations were integrated in time over a grid $0° < \lambda < 45°$ ($0<S<5$). The boundary of the ionosphere corresponds to $\lambda = 65°$, $S = 7.1$. The smaller grid was used since we are interested in propagation through the torus in this instance and the scheme is more economical on a smaller grid. The solutions we obtained are accurate to better than 1%.

Figure 4 (taken from Wright [1986]) shows successive snapshots in time of the wave propagation through the torus. The four panels in each frame correspond to the quantities magnetic field perturbation, plasma flow perturbation, magnetic field displacement and the time-integrated Poynting flux. These quantities are normalized (subscript n) to the magnitude of that quantity for solely the input pulse (subscript on). Thus the input pulse has a field and flow amplitude b_{on} and u_{on}, it produces a displacement of the field line ξ_{on} ($= \int_0^T u_{on}dt$) and it carries an energy density ϵ_{on} ($= \int_0^T u_{on}b_{on}dt$). The sizes of b_{on}, u_{on}, ξ_{on} and ϵ_{on} are indicated on the abscissa by a dash. The pulse in Figure 4 has $T = 0.32$ and should be very similar to the perturbation produced by Io. Let us consider Figure 4a to begin with, taken when $t = 1.0$. The perturbations b_n and u_n are clearly in antiphase, and so the wave is propagating parallel to the magnetic field direction, which is coincident with $\hat{S}$ in this program. It is evident that as the pulse propagates to less dense plasma (i.e., increasing S) the amplitude of b_n decreases, and that of u_n increases. This is in accord with the WKB limit, and we would expect this to apply near the equator where the scale lengths of the medium are much greater than $V_{Aeq}.T$. It is also possible to see that the leading half of the pulse is slightly broader than the trailing half. This is because the Alfvén speed increases monotonically with S. The field line displacement shows very little departure from ξ_{on} near $S = 0$, and it is not until $S \sim 0.7$ that significant increase is found. Thus there is also very little change in the velocity perturbation until $S \sim 0.7$. The time-integrated Poynting flux is constant as far as the pulse has propagated which means that there is negligible reflection in the region $0 < S < 0.7$.

Figure 4b is a snapshot of the same pulse at $t = 1.5$. The time-integrated Poynting flux trace tells us that a little over 20% of the power in the pulse has flowed out of the ionospheric end. The plot of field line displacement shows an increase with S (due to the increase in u_n) followed by a decrease (presumably because not all of the pulse has penetrated the high-latitude region of the field line). The magnetic and velocity field disturbances are not as easy to interpret as those in Figure 4a. This is because they are now a superposition of forward and backward traveling waves. (N.B.: in the linear limit, forward and backward traveling waves do not couple with one another.) The point around $S = 2.2$, where $u_n = 0$ and $b_n \neq 0$, corresponds to forward and backward traveling components of the same magnitude. Equatorward of this point the

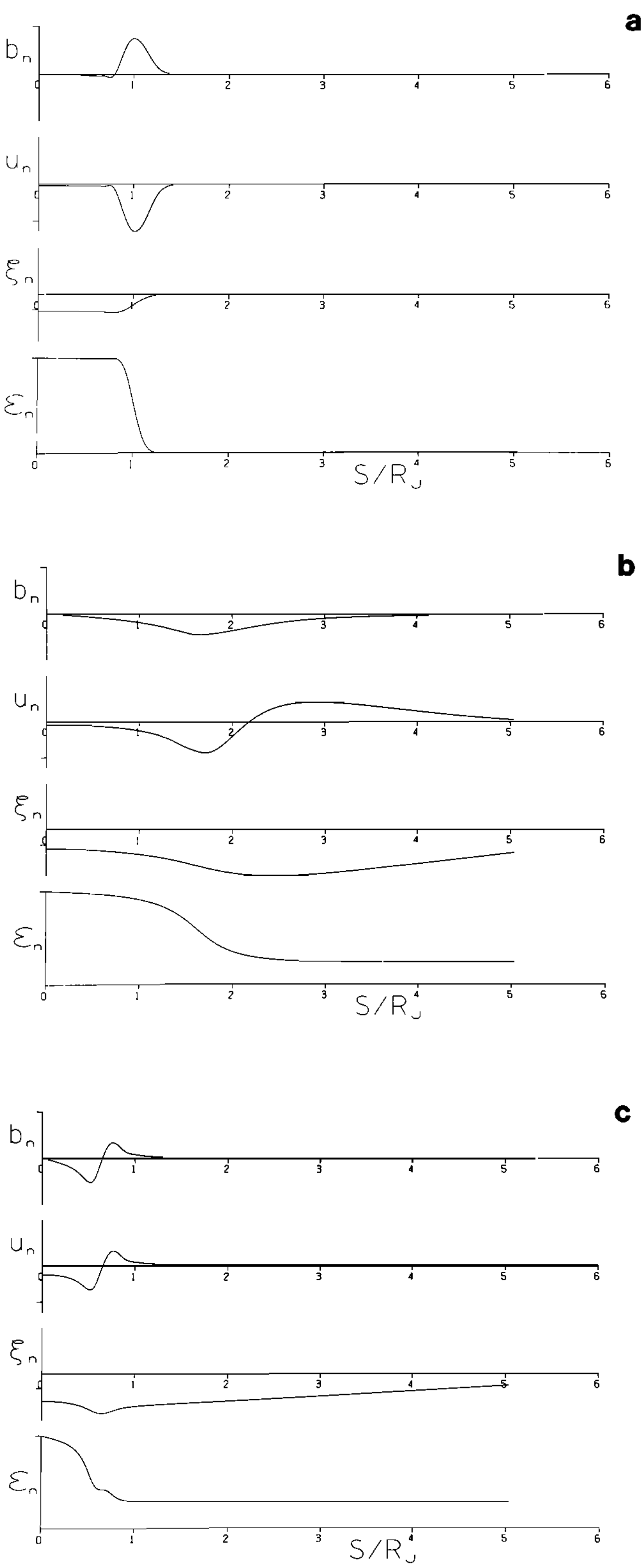

Fig. 4. The propagation of an Alfvén wave through the Io torus. The four panels show the variation of the magnetic field perturbation (b_n); the velocity perturbation (u_n); the field line displacement (ξ_n); and the time-integrated Poynting flux (ϵ_n) with distance along the L shell. S = 0 is at the equator. Each figure is a snapshot in time: (a) t = 1.0; (b) t = 1.5; (c) t = 2.1. The plots are discussed in the text.

equatorward traveling component is larger because the field and flow perturbations are predominantly in phase. Conversely, above S ≃ 2.2 the component traveling toward the ionosphere is the more significant.

Figure 4c is the state of the field line at t = 2.1. The magnetic and velocity field disturbances are clearly largely in phase. This corresponds to an equatorward traveling pulse. There is a similar perturbation in the $S < 0$ space, but with the field perturbation inverted. It is the superposition of these two waves that holds $b_n = 0$ at $S = 0$. The superposition of the waves also causes b_n/u_n to deviate from ± 1 near S = 0. The equatorward traveling pulse has a Poynting flux in the opposite sense to the initial pulse. This can be seen in the integrated Poynting flux trace. The energy that has passed through the plane at S ~ 1.5 when t = 2.1 (Figure 4c) is less than when t = 1.5 (Figure 4b). This is due to the reflected wave transporting energy in the opposite direction to the initial perturbation. The field line above S ~ 1.5 is effectively unperturbed in Figure 4c. If $u_n = 0$, then $\partial\xi_n/\partial t = 0$, and futhermore, (8) tells us that if $b_n = 0$, then $\xi_n h_\alpha B_0$ is independent of S. Thus, from (12) and a dipole B_0, we would expect ξ_n to be proportional to $\cos^3\lambda$. This is consistent with the decreasing magnitude of ξ_n along the field line in the unperturbed region, and shows that the geometric factors are functioning as expected. The energy transmission coefficient can be calculated by taking the ratio of ϵ_n at the end of the field line to ϵ_{on}. This corresponds to the fraction of the input power that propagates through the torus without a reflection from the torus followed by a subsequent penetration.

Several such simulations were carried out for pulse lengths (T) ranging from 0.04 to 5.0 (predicted T = 0.34). The energy transmission coefficient (C_T) for the first pass through the torus was determined and is displayed in Figure 5. The trend between the WKB limit ($C_T \to 1$, $T \to 0$) and the long-wavelength limit ($C_T \to 2\times10^{-4}$, $T \to \infty$) is evident. For the expected pulse duration excited by Io (T ≈ 0.34) we would anticipate an energy transmission coefficient of $C_T \approx 0.25$. The remainder of the energy will be reflected by inhomogeneities in the medium and will propagate toward the equator. Again, only a certain fraction of the wave energy will be transmitted through the medium (how much will depend upon the form of the reflected pulse).

Inspection of Figure 4c shows that the reflected pulse is slightly broader than the input pulse. Subsequent reflections from the medium may broaden this wave packet further.

Discussion and Conclusions

A numerical solution to the single-fluid MHD equations has been presented for an Alfvén wave launched from Io into a dipole geometry with a suitable torus density profile. For waves that have a time scale like that expected to be produced by Io we find a very strong interaction with the inhomogeneities in the medium. The computed solution varies significantly from the WKB solution, which we conclude is inappropriate to describing Io's Alfvén waves. A measure of the departure from this solution is the complete transmission of the wave in the WKB limit and the strong (~75%) reflection produced by our simulation. If the areas of current source on Io are very small, it will be possible to generate Alfvén waves of a small enough wavelength to satisfy the WKB limit. However, a source region that is an order of magnitude smaller than the satellite will only transmit about 75% of its energy on the first pass through the torus (see Figure 5), and so we feel that the WKB limit is never likely to be satisfied. Recent "ray tracing" studies of Alfvén wave propagation assume

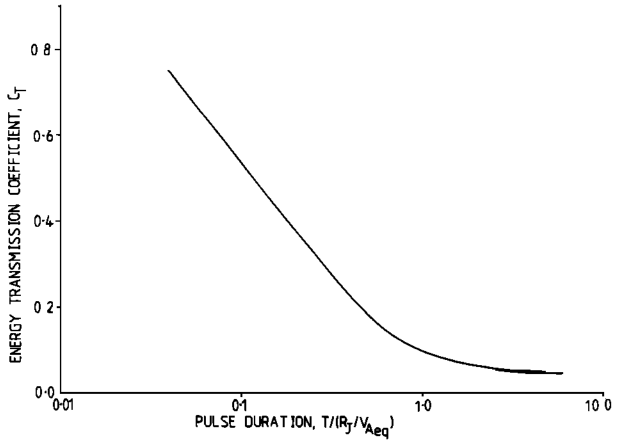

Fig. 5. The dependence of the energy transmission coefficient (C_T) on pulse length is shown. C_T is the fraction of the wave energy that reaches the end of the grid (i.e., field line) on the first pass. The trend between the WKB limit ($T \to 0$, $C_T \to 1$) and the large wavelength limit ($T \to \infty$, $C_T \to 2\times10^{-4}$) is evident.

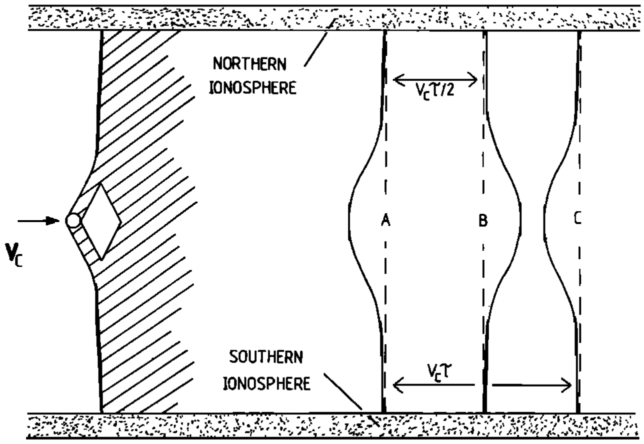

Fig. 6. The Jovian magnetic field is shown schematically bounded by the northern and southern Jovian ionospheres. The plasma flows past Io at V_C, and Alfvén waves propagate along the characteristic directions. The hatched region marks the area disturbed by the new Alfvén wave launched from Io. The disturbance distributes itself along the entire length of the field line and can be described as a superposition of field line eigenmodes. The fundamental eigenmode is shown in the wake of Io and oscillates with a period τ that corresponds to a longitudinal periodicity of $V_C\tau$.

that the WKB limit is valid and that the wave is not reflected within the medium. In the light of these computations this is a dubious assumption, and caution should be exercised. It is found that Neubauer's [1980] conjecture of Alfvén wave reflection from the torus density profile may be of importance. The strong increase in magnetic field strength at higher latitudes may also be responsible for some reflection of the wave.

Most other studies have assumed that the wave propagates completely to the Jovian ionosphere and suffers efficient reflection, thus setting up a stationary wave trajectory behind the satellite (in the satellite frame). In contrast to this we envisage a strong interaction with the medium and expect the wave to undergo reflection and transmission on propagating to the ionosphere. The wave will be well reflected from the ionosphere [Gurnett and Goertz, 1981], but the return wave will also undergo further reflection and transmission by the medium. From the ray tracing standpoint this would produce a complicated standing pattern behind the satellite, which increased in complexity with distance downstream. However, our results show that the pulse is broadened by its interaction with the medium, and so the concepts of ray tracing would necessarily become blurred. Including reflection from the Jovian ionosphere will broaden the pulse even more. From the results in Figure 4 we can estimate that after about 10 bounces the pulse will be so blurred that one may expect a standing mode on the field line to be a more useful way to think of the perturbation launched from Io.

The eigenmodes excited by the passage of Io are beyond the scope of the present paper. However, it is still useful to discuss the basic properties of eigenmodes and their likely implications. We shall now consider the entire field line that is bounded by perfectly reflecting ionospheres. Figure 6 shows the scenario that we may anticipate. The hatched region is disturbed by the Alfvén wave launched from Io. As Neubauer [1980] commented, the only space not influenced by the Alfvén wave is a small diamond shape immediately behind Io where the reflection has not penetrated. The remaining field downstream from Io is disturbed everywhere. Some distance back from Io we have sketched the fundamental eigenmode of the field line. The fundamental mode has a longitudinal periodicity commensurate with the eigenfrequency and the speed of plasma past Io. The field line at line A is at its maximum extent. If the time period of the mode is τ, the field line will have the opposite phase a distance $V_C\tau/2$ downstream (line B) and will have recovered its original phase a distance $V_C\tau$ from line A. The currents (given by curl B) are a maximum at line A, line B and line C, the direction of current flow being opposite in line B to that of line A and line C. The currents could produce DAM in just the same way as ray tracing current structures.

The fundamental mode shown in Figure 6 is not the only mode possible. For example, if Io is off the magnetic equator, it may excite higher eigenmodes particularly. These would have a closer spacing downstream from Io and may explain the 2–3 times too closely spaced arcs (from a ray tracing standpoint) reported by D. H. Staelin et al. (Jovian decametric arcs and Alfvén currents, submitted to Journal of Geophysical Research, 1986, herinafter Staelin et al., 1986). The only way that ray tracing can produce such closely spaced arcs is by the longevity of Alfvén waves produced during previous orbits. From our computations we do not anticipate a long lifetime for the wave packets launched from Io.

In conclusion, we have investigated the propagation of Io's Alfvén waves in the Jovian magnetoplasma. Our numerical results show that the wave interacts strongly with the medium's inhomogeneities. We find that both WKB and ray tracing notions are inappropriate. The motion of field lines that have been perturbed by Io is probably better thought of in terms of field line eigenmodes. In this scenario, Io is a driving force which deposits energy in the eigenmodes. It is hoped that the interpretation of DAM arcs from this new standpoint will explain some of the "anomalous" features found so far. One such feature is the closely spaced arcs (2–3 times the ray tracing periodicity) reported by Staelin et al. [1986].

Appendix

In this appendix we examine the linearized cold plasma equations for an arbitrary field perturbation and background magnetic field. We use the generalized curvilinear coordinate system shown in Figure 1 in which α and β are also the Euler potentials and S is the length along the field line. Both Singer et al. [1981] and Southwood and Hughes [1983] have used such a coordinate system and studied these equations. However, they both consider the equations for harmonic time dependence and a quasi-transverse magnetic field perturbation. We shall not impose these constraints.

Introductory vector analysis books [e.g., Davis and Snider, 1979] give expressions for the vector operations of ∇ in terms of geometrical factors $h_\alpha = \hat{\alpha}/\nabla\alpha$, $h_\beta = \hat{\beta}/\nabla\beta$, etc. We shall make use of their expressions for curl and div. In this fashion we can write Faraday's law as

$$\frac{\partial}{\partial t}\, \mathbf{b} = \nabla_\wedge(\mathbf{u}_\wedge \mathbf{B}_0) = \nabla_\wedge(u_\beta B_0\hat{\alpha} - u_\alpha B_0\hat{\beta})$$

$$= \hat{\alpha}\,\frac{1}{h_\beta}\cdot\frac{\partial}{\partial s}\,(u_\alpha h_\beta B_0)$$

$$+ \hat{\beta}\,\frac{1}{h_\alpha}\cdot\frac{\partial}{\partial s}\,(u_\beta h_\alpha B_0)$$

$$- \hat{s}\,\frac{1}{h_\alpha h_\beta}\left(\frac{\partial}{\partial\alpha}(u_\alpha h_\beta B_0) + \frac{\partial}{\partial\beta}\,(u_\beta h_\alpha B_0)\right) \qquad \text{(A1)}$$

Note how there is no dependence upon u_s. The parallel magnetic field perturbation changes according to

$$\partial b_s/\partial t = -\nabla.(B_0 u_\perp) = -B_0(\nabla.u_\perp) - (u_\perp.\nabla)B_0$$

This will be negligible for a one-dimensional oscillation ($\partial/\partial\alpha = \partial/\partial\beta = 0$). When applying these equations to an incompressible Alfvén wave, or superposition of small-amplitude Alfvén waves, we will satisfy $\nabla.u_\perp = 0$. If the wave is localized perpendicular to the magnetic field such that B_0 does not change appreciably along a streamline, then $(u_\perp.\nabla)B_0 = 0$ also, and so $\partial b_s/\partial t = 0$.

Magnetometer measurements of the disturbance from Io [Acuña et al., 1981] and the wave downstream from Io [Walker and Kivelson, 1981] show that b_s remains very small. In view of the theoretical arguments above and these observations we shall treat the perturbation to the magnetic field as being strictly orthogonal to $\mathbf{B}_0$.

The momentum equation shows that the velocity perturbation perpendicular to $\mathbf{B}_0$ is the only one that changes,

$$(\mu_0\rho/B_0)\,\frac{\partial}{\partial t}\,\mathbf{u} = \hat{\alpha}\,\frac{1}{h_\alpha}\left(\frac{\partial}{\partial s}(b_\alpha h_\alpha) - \frac{\partial}{\partial\alpha}\,b_s\right)$$

$$+ \hat{\beta}\,\frac{1}{h_\beta}\left(\frac{\partial}{\partial s}\,(b_\beta h_\beta) - \frac{\partial}{\partial\beta}\,b_s\right)$$

$$+ 0\,\hat{s} \qquad \text{(A2)}$$

By assuming that the source of Alfvén waves from Io has $b_s \approx 0$ [Acuña et al., 1981] and $u_s \approx 0$, (A1) and (A2) give two decoupled second-order partial differential equations for b_α and b_β (or u_α and u_β). In section 4 the azimuthal (or β) component is shown, and the solutions are given in section 5.

Acknowledgements. The author is grateful to F. Bagenal, S. J. Schwartz and D. J. Southwood for useful discussions. (D.J.S. proposed and conceived the original line of research.) This work was done mainly at Imperial College (under a U.K. SERC Studentship) and completed at Queen Mary College (under a U.K. SERC Fellowship).

The Editor thanks two referees for their assistance in evaluating this paper.

References

Acuña, M. H., F. M. Neubauer, and N. F. Ness, Standing Alfvén wave current system at Io: Voyager 1 obserations, J. Geophys. Res., 86, 8513, 1981.

Acuña, M. H., K. W. Behannon, and J. E. P. Connerney, Jupiter's magnetic field and magnetosphere, in Physics of the Jovian Magnetosphere, edited by A. J. Dessler, Cambridge University Press, New York, 1983.

Alfvén, H., and C.-G. Fälthammar, Cosmical Electrodynamics, Oxford University Press, New York, 1963.

Bagenal, F., Alfvén wave propagation in the Io plasma torus, J. Geophys. Res., 88, 3013, 1983.

Bagenal, F., R. L. McNutt, Jr., J. W. Belcher, H. S. Bridge, and J. D. Sullivan, Revised ion temperatures for Voyager plasma measurements in the Io plasma torus, J. Geophys. Res., 90, 1755, 1985.

Barnett, A. S., In situ measurements of the plasma bulk velocity near the Io flux tube, J. Geophys. Res., 91, 3011, 1986.

Belcher, J. W., C. K. Goertz, J. D. Sullivan, and M. H. Acuña, Plasma observations of the Alfvén wave generated by Io, J. Geophys. Res., 86, 8508, 1981.

Bigg, E. K., Influence of the satellite Io on Jupiter's decametric emission, Nature, 203, 1008, 1964.

Davis, H. F., and A. D. Snider, Introduction to Vector Analysis, Allyn and Bacon, London, 1979.

Dessler, A. J. (Ed.) Physics of the Jovian Magnetosphere, Cambridge University Press, New York, 1983.

Drell, S. D., H. M. Foley, and M. A. Ruderman, Drag and propulsion of large satellites in the ionosphere, J. Geophys. Res., 70, 3131, 1965.

Goertz, C. K., Io's interaction with the plasma torus, J. Geophys. Res., 85, 2949, 1980.

Goertz, C. K., and P. A. Deift, Io's interaction with the magnetosphere, Planet. Space Sci., 21, 1399, 1973.

Goldreich, P., and D. Lynden-Bell, Io, a Jovian unipolar inductor, Astrophys. J., 156, 59, 1969.

Goldstein, B. E., and W.-H. Ip, Magnetic drifts at Io: Depletion of 10-MeV electrons at Voyager 1 encounter due to a forbidden zone, J. Geophys. Res., 88, 6137, 1983.

Gurnett, D. A., and C. K. Goertz, Multiple Alfvén wave reflections excited by Io: Origin of the Jovian decametric arcs, J. Geophys. Res., 86, 717, 1981.

Lanzerotti, L. J., C. G. MacLennan, T. P. Armstrong, S. M. Krimigis, R. P. Lepping, and N. F. Ness, Ion and electron angular distributions in the Io torus region of the Jovian magnetosphere, J. Geophys. Res., 86, 8491, 1981.

Neubauer, F. M., Nonlinear standing Alfvén wave current system at Io: Theory, J. Geophys. Res., 85, 1171, 1980.

Schulz, M., and A. Eviatar, Charged particle absorption by Io, Astrophys. J. Lett., 211, L149, 1977.

Singer, H. J., D. J. Southwood, R. J. Walker, and M. G. Kivelson, Alfvén wave resonances in a realistic magnetospheric magnetic field geometry, J. Geophys. Res., 86, 4589, 1981.

Southwood, D. J., and M. W. Dunlop, Mass pickup in sub-Alfvénic plasma flow: A case study for Io, Planet. Space Sci., 32, 1079, 1984.

Southwood, D. J., and W. J. Hughes, Theory of hydromagnetic waves in the magnetosphere, Space Sci. Rev., 35, 301, 1983.

Walker, R., and M. G. Kivelson, Multiply reflected standing Alfvén waves in the Io torus: Pioneer 10 observations, Geophys. Res. Lett., 8, 1281, 1981.

Warwick, J. W., J. B. Pearce, A. C. Riddle, J. K. Alexander, M. D. Desch, M. L. Kaiser, J. T.

Thieman, T. D. Carr, S. Gulkis, A. Boischot, Y. Leblanc, B. M. Pedreson, and D. H. Staelin, Planetary radio astronomy observations from Voyager 2 near Jupiter, Science, 206, 991, 1979a.

Warwick, J. W., J. B. Pearce, A. C. Riddle, J. K. Alexander, M. D. Desch, M. L. Kaiser, J. R. Thieman, T. D. Carr, S. Gulkis, A. Boischot, C. C. Harvey, and B. M. Pederson, Voyager 1 planetary radio astronomy observations near Jupiter, Science, 204, 995, 1979b.

Wright, A. N., The plasma physics of Io and its neighbourhood, Ph.D. thesis, Univ. of London, 1986.

Wright, A. N., Energetic particle absorption at Io, J. Geophys. Res., 92, 3155, 1987.

Wright, A. N. and D. J. Southwood, Stationary Alfvénic structures, J. Geophys. Res., 92, 1167, 1987.

A. N. Wright, Theoretical Astronomy Unit, Queen Mary College, University of London, Mile End Road, London, E1 4NS, England.

(Received December 1, 1986;
revised May 22, 1987
accepted May 27, 1987.)